Egypt. J. Chem. **Vol. 66**, No. SI: 13 pp. 551 - 560 (2023)

Egyptian Journal of Chemistry

http://ejchem.journals.ekb.eg/

Bioresoursed Nano-Sio$_2$/Styrene-Co-Vinyl Acetate Nano-Composite: Synthesis, Characterization and Evaluation as Nano-Pour Point Depressant and Paraffin Inhibitor for Waxy Crude Oil

Sameh A. Elbanna[a], Hanan A. Ahmed[b,*]

[a] *Processes Development Department, Egyptian Petroleum Research Institute, Nasr City, Cairo 11727, Egypt*

[b] *Petrochemicals Department, Egyptian Petroleum Research Institute, Nasr City, Cairo 11727, Egypt*

Abstract

The problem of wax precipitation and deposition in crude oils at low temperatures causes severe problems in the petroleum industry. Among the various developed approaches to solve this issue is the injection of polymer nano-composites into waxy crude oil. Herein, the bagasse of sugarcane waste as a bioresource was used for silica nano-particles (Nano-SiO_2) extraction. Also, a new copolymer of styrene-co-vinyl acetate was prepared then, a novel nano-composite; Nano-SiO_2/styrene-co-vinyl acetate composed of the produced bioresoursed Nano-SiO_2 and styrene-co-vinyl acetate was prepared. Fourier transform infrared spectroscopy, X-ray diffraction, scanning electron microscopy, transmission electron microscopy, and gel permeation chromatography analytical techniques were used to characterize the produced materials. Additionally, the synthesized Nano-SiO_2/styrene-co-vinyl acetate was applied as a cheap nano-pour point depressant and paraffin inhibitor for the waxy crude oil and its performance was compared with the pristine styrene-co-vinyl acetate copolymer. Various concentrations (100 ppm-800 ppm) of the synthesized additives were injected into the collected crude oil samples at 60 ºC. The results indicated that the dosages of the injected pour point depressants have a significant impact on their performance. Optimum dosages of 400 ppm and 600 ppm of Nano-SiO_2/styrene-co-vinyl acetate and styrene-co-vinyl acetate respectively were found to be efficient in depressing the pour point temperature and inhibiting the paraffins aggregation at low temperatures.

Keywords: Synthesis and characterization; Nano-silica; Polymer nano-composite; Nano-pour point depressant; Paraffin inhibitor; Waxy crude oil

1. Introduction

By advancing agribusiness, there is an increase in the raw materials consumption and production of agricultural and agro-industrial wastes. Thus, special interest has been focused on minimizing these effluents and their reuse via converting biomass-derived wastes to highly added value-materials [1]. Potential low cost waste products obtained due to agricultural and industrial activities may be efficient alternatives for the application in various fields. For example, fly ash waste [2], husk of rice [3], bones of animals [4], nutshells [5], olive-waste cakes [6], and bagasse waste (SB) [7, 8] are recently used for preparing cost effective materials and tested for various valuable applications. Among the mentioned wastes, sugarcane bagasse is a solid waste produced in huge amounts annually throughout the world as a byproduct of cane sugar stalks left over after rushing to extract the juice from sugarcane [9, 10]. A previous study [11] showed that the process of bagasse combustion produces high amounts of inorganic components such as silica accompanied by small amounts of iron, aluminum, alkalis, and alkaline earth oxides. However, the combustion treatment requires high energy consumption, and this has prevented the widespread commercial use of this waste material [10, 12, 13]. This waste was also used to prepare nano-silica and glass-ceramic materials,

*Corresponding author e-mail: drhananepri@yahoo.com.; (Hanan A. Ahmedb).
EJCHEM use only: Received date 19 December 2022; revised date 25 February 2023; accepted date 05 March 2023
DOI: 10.21608/EJCHEM.2023.181813.7351

respectively [14, 15]. Moreover, due to the existence of high content of amorphous SiO_2 in this waste it was utilized as a source of silica for the production of water glass material [16]. Due to the sustainability, low cost and availability of bio-resourced based silica materials, they are receiving crescent attention in different promising applications including energy storage [17], energy production [3], catalysis [8, 18], and wastewater treatment [19].

Enhancing polymeric materials' performance by incorporating inorganic substances has an important industrial activity and has been achieved by using materials such as talc, carbon blacks, clays, and silica [20-22]. With the rapid development of nanotechnology in recent years, nano-composite materials have been applied in crude oil production and transportation [23, 24]. The utilization of nano-scale materials produces polymer nano-composites with enhanced properties including mechanical and dielectric properties [25-27] due to the unique high adsorption affinity of nanoparticles [28-35]. Wang et al. [36] have introduced nano-MMT clay into polymer matrices' pour-point depressants (PPDs) to form polymer/nano-MMT PPDs of improved performances. Crude oil with a high content of wax often exhibits a high wax apparent temperature (WAT) [37]. Below this temperature, the crude oil loses its flow characteristics and is defined as the crude oil's pour point at which the wax molecules begin to precipitate, overlap and interlock to form a three-dimensional network structure in the oil phase [38]. Thus, this will reduce the mobility of crude oil. The precipitation and deposition of wax crystals at low temperatures cause severe problems in oil production, storage, and transportation [37-39]. Many approaches have been developed to overcome those problems. While, due to the high cost and energy consumption of these methods, the chemical approaches, particularly the addition of polymeric pour-point depressant (PPD) is usually cost-effective and time saving [40]. It was commonly accepted that PPD can effectively change the structure and dispersity of wax crystals and prohibit the formation of rigid networks at low temperatures [41]. Among the economical and effective conventional PPDs, ethylene-vinyl acetate copolymers [42-47], α-olefin polymers [37], maleic anhydride copolymers and their derivatives are widely used [38-40]. The current research aim is adapted as follows: The waste bagasse was utilized as a resource to extract bioresoursed nano-silica. A new polymeric additive; styrene-co-vinyl acetate was prepared, then; an environmentally friendly industrial product of Nano-SiO_2/styrene-co-vinyl acetate nano-composite was synthesized. Also, the prepared samples were characterized by various techniques including Fourier transform infrared spectroscopy, X-ray diffraction, scanning electron microscopy, transmission electron microscopy, and gel permeation chromatography. Moreover, styrene-co-vinyl acetate and Nano-SiO_2/styrene-co-vinyl acetate nano-composite were injected by various dosages (100 ppm, 200 ppm, 400 ppm, 600 ppm and 800 ppm) into Tut-waxy crude oil samples to be evaluated as novel pour point depressants (PPDs) and paraffin inhibitors (PIs).

2. Materials and Methods

2.1. Materials

The Styrene and vinyl acetate (Reagent grades, Beijing Yanshan Petroleum Chemical Co) were distilled before usage as described before [48]. Benzoyl peroxide and xylene were used as supplied as the initiator and solvent, respectively. All chemicals utilized to extract nano-silica from the bagasse including sodium hydroxide, hydrochloric acid, and ammonium hydroxide was used as bought from Merck.

2.2. Methods

2.2.1. Bioresoursed Nano-SiO_2 Extraction from Sugarcane Bagasse

Sugarcane bagasse waste was collected from sugarcane juice industries in Cairo, Egypt, washed repeatedly with tap water, dried under the sun until complete dryness, chipped into small pieces, ground, and sieved into 150 μm. The ground bagasse was pyrolyzed at 660 ^{o}C (6 ^{o}C/min) for 3 h to obtain the bagasse ash (BA). Then, the BA was treated with 1 mol/L HCl as follows: 10 g of BA was stirred with 100 ml of 1 mol/L HCl for 4 h at 25 ^{o}C. The suspension was filtered and the solid residue was washed with distilled water to remove the metallic ions. The residue was then dried at 80 ^{o}C for 24 h to be used for sodium silicate preparation. The obtained ash residue was dispersed in 100 ml of 3 mol/L NaOH solution for 3 h at 95 ^{o}C under stirring (750 rpm). After that, the solid residue was eliminated from the obtained suspension via filtration. The resulting filtrate (sodium silicate solution) was then used as a precursor for Nano-SiO_2 extraction. It was titrated with 1 mol/L NH_4OH until the formation of gel which was aged at 45 ^{o}C for 14 h, washed, filtered, and dried at 90 ^{o}C overnight to obtain a white powder of SiO_2 nano-particles.

2.2.2. Preparation of Styrene-Co-Vinyl Acetate

Styrene copolymerization with vinyl acetate (with a molar ratio of 1: 1) was initiated by benzoyl peroxide in a solvent of xylene at 70 °C for 5 h under N_2 atmosphere. The styrene-co-vinyl acetate (PSV) copolymer was then precipitated with methanol and dried under vacuum [49].

2.2.3. *Synthesis of Nano-SiO_2/ Styrene-Co-Vinyl Acetate Nano-Composite*

The synthesis of Nano-SiO_2/styrene-co-vinyl acetate (Nano-SiO_2/PSV) nano-composite was done by the hybridization of the waste bagasse extracted Nano-SiO_2 with PSV copolymer. The solution blending method described in a previous study [50] was used to do this hybridization. An equal mass ratio of 1: 1 Nano-SiO_2: PSV was applied for the synthesis of the nano-composite. Firstly, 1 g of PSV copolymer was dissolved in 40 ml of toluene then, 1 g of Nano-SiO_2 was dispersed into the copolymer/toluene solution by ultrasonic treatment for 30 min at 25 °C until a homogeneous solution formation. After that, the solution was heated to 78 °C under continuous stirring for 3 h. Finally, the toluene solvent was removed by continuous stirring and evaporation at 120 °C to produce the nano-PPD and PI (Nano-SiO_2/PSV nano-composite) as represented in Fig. 1.

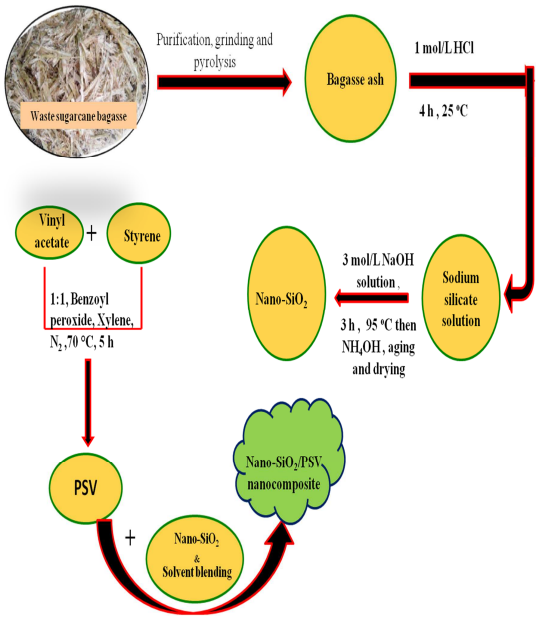

Figure 1: Nano-SiO_2/PSV nano-composite synthesis diagram

2.3. *Characterization*

Fourier Transform Infrared (FTIR) spectroscopical analysis was used to confirm the structure of bagasse, Nano-SiO_2, PSV, and Nano-SiO_2/PSV samples using Nicolet IS-10 FTIR over the wavenumber range of 4000–400 cm^{-1} [51]. X-ray diffraction (XRD) was employed using X'Pert PRO PANalytical diffractometer [52]. The reflections were monitored using CuKα radiation at λ = 0.1541 nm and 2θ ranged from 5° to 65°. The surface morphology of the samples was carried out by scanning electron microscopy (SEM, JEOL, JSM-6700F system) [51]. Gel permeation chromatography (GPC) was used to evaluate the average molecular weights (Mw and Mn) of the prepared PSV copolymer using GPC-Water 2410 with a refractive index detector [38-40]. Transmission electron microscopy (TEM, Model JEM-200CX, JEOL 2100, Japan) operated at 200 kV was done for the extracted SiO_2 to investigate its size and morphology [53].

2.4. *Nano-SiO_2/PSV Evaluation as A Nano-PPD for Tut-Waxy Crude Oil*

The synthesized Nano-SiO_2/PSV nano-composite and PSV copolymer were assessed as PPDs with different concentrations (100, 200, 400, 600, 800 ppm) and injected into the heated waxy-oil samples which were heated to 60 ºC. The injected samples were continuously stirred (350 rpm) for 30 min then ultrasonicated for 30 min to ensure complete dissolution and uniform dispersion of these additives in the waxy crude oil. Thereafter, the un-injected and injected crude oil samples were evaluated by applying the ASTM D97 [52, 54, 55].

2.5. *Nano-SiO_2/PSV Evaluation As A Nano-PI for Tut-Waxy Crude Oil*

The Cold Finger experiment was performed at the Chemical Services and Development Center, EPRI, Cairo, Egypt to evaluate the impact of PSV copolymer and Nano-SiO_2/PSV nano-composite as PIs. This model is used as a convenient way to simulate the wax precipitation process inside the oil pipeline according to the method described in previous studies [37, 56]. After the mentioned method completion, the residual deposition of wax was gradually removed from the cold finger and measured.

2.6. *Waxy Crude Oil Analysis*

Tut-waxy crude oil was collected from Khalda Petroleum Company fields, in the Western Desert, Egypt. Its physico-chemical characteristics were identified as displayed in Table 1. Also, waxes and asphaltene were isolated and their quantity was determined by applying the UOP method (46/64) and the IP 143/84, respectively [38].

3. Results and Discussion

3.1. *Crude Oil Characterization*

The physico-chemical features of Tut-waxy crude oil are displayed in Table 1. From these results, we can reveal the waxy nature (13 wt% wax content) of the obtained crude oil.

Table 1
Physical characteristics of the evaluated Tut waxy crude oil

Properties	Method	Result
Density at 20 °C (g/cm^3)	ASTM D1298	0.830
Kinematic viscosity at 40 °C cst	ASTM D445	2.77
Dynamic viscosity at 40 °C cp	ASTM D2196-18	2.30
Pour point (PP), °C	ASTM D 97	27.0
Wax content, (wt %)	UOP 46/64	13.0
Asphaltene content, (wt %)	IP 143/84	2.00
Average carbon number (n)	IP 372/85	12.34
Water content, (wt %)	IP 74/70	0.35
Ash content, (wt %)	ASTM D 482	0.02
API gravity at 60° F	ASTMD-1298	38.96

3.2. *Samples Characterization*

3.2.1. *FTIR Spectra*

The FTIR spectra of waste bagasse (WB), bioresoursed Nano-SiO_2, PSV, and Nano-SiO_2/PSV nano-composite are presented in Fig. 2. In the WB spectrum there is an absorption band centered at 3357 cm^{-1} indicates the existence of free and intermolecular bonded hydroxyl groups [57, 58]. The broad FTIR-band centered at 2902 cm^{-1} can be assigned to the stretching vibration of the C–H group [54]. The two bands detected at 1734 cm^{-1} and 1053 cm^{-1} correspond, respectively to the C= C stretching and –OCH_3 group that existed in the lignin aromatic groups of baggase. The other two bands detected at 604 and 830 cm^{-1} can be assigned to the bending modes of aromatic compounds [59]. The FTIR spectrum of baggase nano-silica (Fig. 2) shows the FTIR-bands of Si–O–Si asymmetry stretching, Si–O symmetric bending and stretching, and the H–O–H bending vibration characteristics of silica which detected, respectively at 1089 cm^{-1}, 467 cm^{-1} and 794 cm^{-1}, and at 1637 cm^{-1} [3, 12, 54]. The asymmetric stretching and bending vibrations of silanol OH groups are detected at 3494 cm^{-1} [60] while the bending mode of Si-O and the adsorbed water band is observed at 475 cm^{-1} and 963 cm^{-1} [3, 53, 55]. The successful copolymerization of PSV was elucidated by FTIR spectroscopy (Fig. 2). From Fig. 2, the FTIR-bands of CH_3-, -CH_2- [61], and the phenyl –C_6H_5 protons of styrene [49] are detected at 2920 cm^{-1}, 2854 cm^{-1} and 3026 cm^{-1}, respectively. Also, the aromatic C─H vibrations deforming in the benzene ring of styrene and the -CH_2- of the side vinyl group are detected at 696-1491 cm^{-1} region [62, 63]. Additionally, the two bands detected at 1236 cm^{-1} and 1730 cm^{-1} are attributed to the ester groups stretching vibrations of vinyl acetate [64-66]. The above-discussed FTIR-bands for the PSV spectrum besides the absence of any bands at ~1605 cm^{-1} which characterize the non-conjugated (C=C str)-band and the existence of polymeric backbone CH_2- at 720 cm^{-1} implies the successful preparation of PSV copolymer. By comparing the FTIR spectrum of Nano-SiO_2/PSV nano-composite with those of Nano-SiO_2 and PSV copolymer (Fig. 2), there are three FTIR-bands assigned to Nano-SiO_2 detected at the wavenumbers of 1136 cm^{-1}, 1647 cm^{-1} and 3439 cm^{-1} in the nano-composite spectrum. Additionally, there is a decrease in the intensity of the ester group bands and some shifts in the vibrations of PSV relative to the nan-composite approving the successful synthesis of Nano-SiO_2/PSV nano-composite.

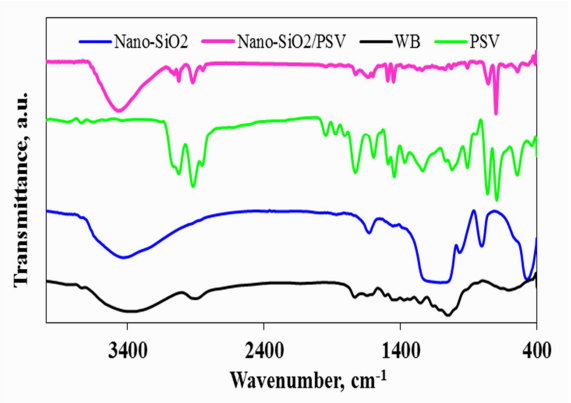

Figure 2: FTIR spectra of WB, Nano-SiO_2, PSV, and Nano-SiO_2/PSV

3.2.2. XRD Results

The phase determination of the bioresoursed Nano-SiO_2 and the synthesized Nano-SiO_2/PSV nano-composite examined by XRD analysis are presented in Fig. 3. The extracted nano-SiO_2 XRD patterns (Fig. 3) showed a broad peak between the 2θ of 17.49° and 26.35° implying that the SiO_2 nanoparticles are in the amorphous form [3]. While the XRD patterns of Nano-SiO_2/PSV presented some crystalline reflections besides the amorphous nano-SiO_2 broad peak existence confirming the successful synthesis of the nano-composite.

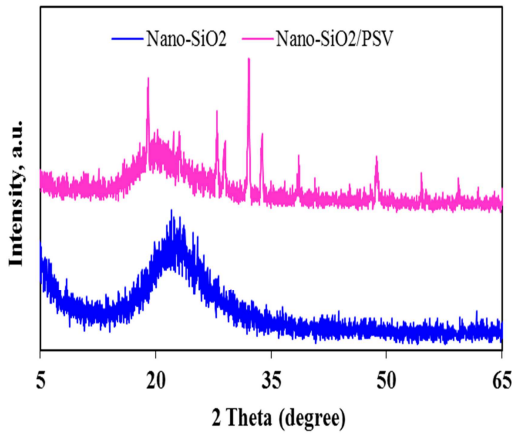

Figure 3: XRD patterns of Nano-SiO_2 and Nano-SiO_2/PSV

3.2.3. TEM and SEM Analysis

The morphology of the extracted Nano-silica examined by TEM is shown in Fig. 4a. It was found that the particles of the extracted silica are of spherical shape and are in the nanometer scale with the size range of 7.11-10.39 nm.

Additionally, the surface morphology of Nano-silica and Nano-SiO_2/PSV nano-composite examined by SEM are shown in Fig. 4b and c. The SEM image of SiO_2 indicates its consistence of agglomerated spherical particles. While the Nano-SiO_2/PSV nano-composite image shows that it has an irregular shape besides the presence of some SiO_2 spherical particles distributed randomly on the copolymer surface and other particles clustered with a non-uniform and rough surface.

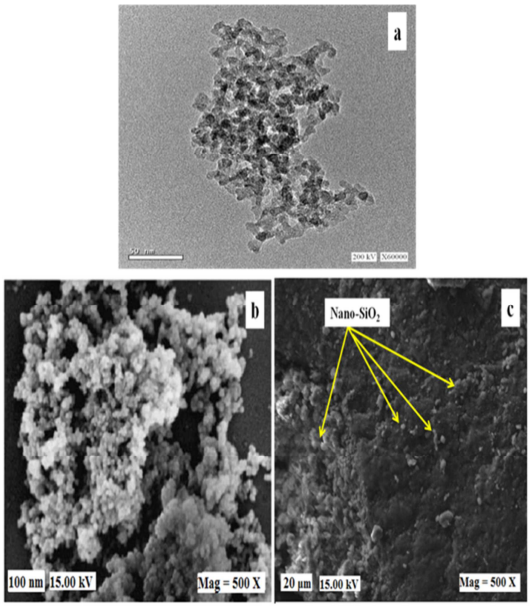

Figure 4: a) TEM of Nano-SiO_2, b) SEM of Nano-SiO_2 and c) SEM of Nano-SiO_2/PSV

3.2.4. GPC Analysis for PSV Copolymer

The weight average and number average molecular weights (Mw and Mn) of PSV copolymer are tabulated in Table 2. It was found that the PSV copolymer has Mn and Mw of 19818 g/mol and 68437 g/mol, respectively revealing the successful copolymerization of styrene with vinyl acetate to form PSV copolymer.

Table 2
Average molecular weights for PSV copolymer

Sample abbreviation	M_n (g/mol)	M_W (g/mol)
PSV	19818	68437

3.3. PSV and Nano-SiO_2/PSV Evaluation as PPDs for Waxy Crude Oil

The results of PSV and Nano-SiO_2/PSV injection on the pour point temperature (PPT, ºC) of the waxy crude oil are listed in Table 3. It's obvious that the pour point depression of the injected crude oil was enhanced by increasing the dosages of PSV and Nano-SiO_2/PSV, respectively to 600 ppm and 400 ppm relative to the non-injected one. The PPD values were constant above these dosages. Thus, 600 ppm of

PSV copolymer and 400 ppm of Nano-SiO_2/PSV nano-composite should be considered as the optimum dosages which reduced the pour point temperature of Tut-waxy crude oil from 27 ºC (crude oil blank) to 12 ºC and 6 ºC, respectively.

Table 3
Effect of injecting different dosages of PSV copolymer and Nano-SiO_2/PSV nano-composite on the PPD of Tut-waxy crude oil

Additive dosage, (ppm)	Pour point depression (°C), PPT		
	Blank	PSV	Nano-SiO_2/PSV
100	27	21	18
200	27	18	12
400	27	15	6
600	27	12	6
800	27	12	6

The results also indicate that the produced Nano-SiO_2/PSV is a better PPD than PSV for the waxy crude oil which may be ascribed to the presence of nano-silica in the nano-composite which contains a lone pair of electrons making it able to adsorb on the surface of wax by delocalization and hindering the wax crystal aggregation. Also, the existence of polar silanol (Si─OH) groups at the SiO_2 nano-particles surface beside the polarity of the styrene phenyl group and the ester group of vinyl acetate makes the Nano-SiO_2/PSV more polar than PSV. Thus, the injection of a lower dosage of nano-SiO_2/PSV resulted in better depression for the pour point temperature than the PSV copolymer as mentioned above.

3.4. PSV and Nano-SiO_2/PSV Evaluation as PIs

Figure 5 presents the impact of PSV and Nano-SiO_2/PSV as PIs for Tut-waxy crude oil. This Figure declares that a 9.5 g of wax deposits were isolated from the Tut- waxy oil which were reduced to 2.41 g and 1.13 g after injecting the waxy oil with the optimum dosages; 600 ppm and 400 ppm of PSV and nano-SiO_2/PSV, respectively. The existence of surface polar Si-OH groups onto SiO_2 nano-particles and the styrene phenyl group polarity are the main reasons for the high efficiency of the prepared additives. Thus, the crude paraffins were inhibited by 74.6% and 88.1% as a result of PSV and Nano-SiO_2/PSV injection indicating that both of the mentioned additives can be considered highly efficient and promising paraffin inhibitors for the waxy-crude oil.

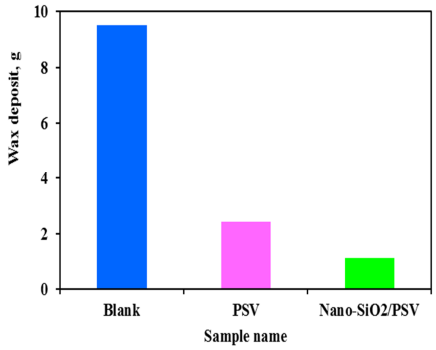

Figure 5: Wax deposition for the blank and the injected crude oil samples

3.5. Comparing the PPD and PI Results of PSV and Nano-SiO_2/PSV with Other Works

As observed from Table 4, the prepared PSV copolymer and Nano-SiO_2/PSV nano-composite were evaluated as PPDs and PIs for waxy crude oil, and the obtained data are compared with the findings of other studies. As shown, Nano-SiO_2/PSV nano-composite is superior to most of the evaluated additives indicating the ability of its utilization as an environmentally friendly competitive nano-PPD and PI additive

Table 4
Comparison of the PPD and PI results of the current study additives with other additives

Additive Name	Additive dosage, (ppm)	PPD (°C)	PI%	Reference
PMMA	1500	28	--	[67]
PMMA-1% GO	1500	15	--	[67]
IHA	200	9	90	[68]
Am_2	2000	6	80	[37]
EVA	200	25.6	--	[69]
IOA	200	12	88	[39]
EVA/nano-MMT	1000	23	--	[70]
Nano-SiO_2/PSV	400	6	88.1	This work
PSV	600	12	74.6	This work

Note: PMMA is poly methyl methacrylate, GO is graphene oxide, IHA is styrene hexadecyl acrylate maleic anhydride imide, Am_2 is Octadecene-styrene amide, EVA is ethylene vinyl acetate, IOA is styrene

octadecyl acrylate maleic anhydride imide, nano-MMT is nano montmorillonite.

4. Conclusions

In this research, the waste bagasse was utilized as an alternative biomass resource for the production of Nano-SiO_2. Also, a new copolymer; styrene-co-vinyl acetate was prepared then, a novel eco-friendly Nano-SiO_2/PSV nano-composite was synthesized. The Nano-SiO_2/PSV nano-composite was evaluated as a nano-PPD and PI for Tut-waxy crude oil and its performance was compared with that of the PSV copolymer. Various analysis including FTIR, XRD, SEM, TEM, and GPC were performed to confirm the successful extraction of spherical amorphous Nano-SiO_2 from the WB, the copolymerization of styrene with vinyl acetate, and the formation of Nano-SiO_2/PSV nano-composite. The PPD results indicated that the injection of 400 ppm and 600 ppm of Nano-SiO_2/PSV and PSV copolymer, respectively into Tut-waxy crude oil reduced the pour point temperature from 27 ºC (crude oil blank) to 6 ºC and 12 ºC. Also, these optimum dosages injection achieved a PI of 88.1% and 74.6%, respectively. This enhancement was due to the synergistic effect of the co-crystallization between PSV and wax crystals and the Nano-SiO_2 which inhibited the growth and precipitation rate of wax crystals in crude oil. So, the current study provides PSV copolymer and Nano-SiO_2/PSV synthetic polymer nano-composite with dual function as promising and efficient PPDs and PIs for the waxy crude oil.

5. Conflict of Interest:

"There are no conflicts to declare".

6. Formatting of funding sources:

"This research did not receive any specific grant from funding agencies in the public, commercial, or not-for-profit sectors".

7. Acknowledgments

"Not applicable".

8. References

[1] Garcia C.F.H., Souza R.B.d., de Souza C.P., Christofoletti C.A., Fontanetti C.S., Toxicity of two effluents from agricultural activity: Comparing the genotoxicity of sugar cane and orange vinasse, Ecotoxicol. Environ. Saf. 142 (2017) 216-221. doi: 10.1016/j.ecoenv.2017.03.053.

[2] Panday K.K., Prasad G., Singh V.N., Copper(II) removal from aqueous solutions by fly ash, Water Research 19(7) (1985) 869-873. doi: 10.1016/0043-1354(85)90145-9.

[3] Awadallah A.E., Solyman S.M., Aboul-Enein A.A., Ahmed H.A., Aboul-Gheit N.A.K., Hassan S.A., Effect of combining Al, Mg, Ce or La oxides to extracted rice husk nanosilica on the catalytic performance of NiO during COx-free hydrogen production via methane decomposition, International Journal of Hydrogen Energy 42(15) (2017) 9858-9872. doi: 10.1016/j.ijhydene.2017.03.049.

[4] Al-Asheh S., Banat F., Mohai F., Sorption of copper and nickel by spent animal bones, Chemosphere 39(12) (1999) 2087-2096. doi: 10.1016/s0045-6535(99)00098-3.

[5] Toles C.A., Marshall W.E., Johns M.M., Phosphoric acid activation of nutshells for metals and organic remediation: process optimization, Journal of Chemical Technology & Biotechnology 72(3) (1998) 255-263. doi: 10.1002/(sici)1097-4660(199807)72:3<255::aid-jctb890>3.0.co;2-p.

[6] Baçaoui A., Yaacoubi A., Dahbi A., Bennouna C., Phan Tan Luu R., Maldonado-Hodar F.J., Rivera-Utrilla J., Moreno-Castilla C., Optimization of conditions for the preparation of activated carbons from olive-waste cakes, Carbon 39(3) (2001) 425-432. doi: 10.1016/s0008-6223(00)00135-4.

[7] Mohan D., Singh K.P., Single- and multi-component adsorption of cadmium and zinc using activated carbon derived from bagasse—an agricultural waste, Water Research 36(9) (2002) 2304-2318. doi: 10.1016/s0043-1354(01)00447-x.

[8] Aboul-Enein A.A., Awadallah A.E., Solyman S.M., Ahmed H.A., Green synthesis of carbon nanomaterials from sugarcane bagasse using bio-silica supported bimetallic nickel-based catalysts, Fullerenes, Nanotubes and Carbon Nanostructures 30(7) (2021) 767-776. doi: 10.1080/1536383x.2021.2023133.

[9] Gupta C.K., Sachan A.K., Kumar R., Examination of Microstructure of Sugar Cane Bagasse Ash and Sugar Cane Bagasse Ash Blended Cement Mortar, Sugar Tech 23(3) (2021) 651-660. doi: 10.1007/s12355-020-00934-8.

[10] Rossignolo J.A., Borrachero M.V., Soriano L., Payá J., Influence of microwave oven calcination on the pozzolanicity of sugar cane bagasse ashes (SCBA) from the cogeneration industry, Construction and Building Materials 187 (2018) 892-902. doi: 10.1016/j.conbuildmat.2018.08.016.

[11] Souza A.E., Teixeira S.R., Santos G.T.A., Costa F.B., Longo E., Reuse of sugarcane bagasse ash (SCBA) to produce ceramic materials, J. Environ. Manage. 92(10) (2011) 2774-2780. doi: 10.1016/j.jenvman.2011.06.020.

[12] Cordeiro G.C., Kurtis K.E., Effect of mechanical processing on sugar cane bagasse ash pozzolanicity, Cement and Concrete Research 97 (2017) 41-49. doi: 10.1016/j.cemconres.2017.03.008.

[13] Ribeiro D.V., Morelli M.R., Effect of Calcination Temperature on the Pozzolanic Activity of Brazilian Sugar Cane Bagasse Ash (SCBA), Materials Research 17(4) (2014) 974-981. doi: 10.1590/s1516-14392014005000093.

[14] Sivakumar G., Amutha K., Hariharan V., Structural and morphological studies on nanosilica from treated bagasse and Rice straw, International Conference on Nanoscience, Engineering and Technology (ICONSET 2011), IEEE, 2011. http://dx.doi.org/10.1109/iconset.2011.6167930
[15] Teixeira S.R., Magalhães R.S., Arenales A., Souza A.E., Romero M., Rincón J.M., Valorization of sugarcane bagasse ash: Producing glass-ceramic materials, J. Environ. Manage. 134 (2014) 15-19. doi: 10.1016/j.jenvman.2013.12.029.
[16] Moubarik A., Grimi N., Boussetta N., Pizzi A., Isolation and characterization of lignin from Moroccan sugar cane bagasse: Production of lignin–phenol-formaldehyde wood adhesive, Industrial Crops and Products 45 (2013) 296-302. doi: 10.1016/j.indcrop.2012.12.040.
[17] Shen Y., Rice Husk Silica-Derived Nanomaterials for Battery Applications: A Literature Review, J. Agric. Food Chem. 65(5) (2017) 995-1004. doi: 10.1021/acs.jafc.6b04777.
[18] Adam F., Appaturi J.N., Iqbal A., The utilization of rice husk silica as a catalyst: Review and recent progress, Catalysis Today 190(1) (2012) 2-14. doi: 10.1016/j.cattod.2012.04.056.
[19] Ahmaruzzaman M., Gupta V.K., Rice Husk and Its Ash as Low-Cost Adsorbents in Water and Wastewater Treatment, Industrial & Engineering Chemistry Research 50(24) (2011) 13589-13613. doi: 10.1021/ie201477c.
[20] He C., Ding Y., Chen J., Wang F., Gao C., Zhang S., Yang M., Influence of the nano-hybrid pour point depressant on flow properties of waxy crude oil, Fuel 167 (2016) 40-48. doi: 10.1016/j.fuel.2015.11.031.
[21] Jing G., Sun Z., Tu Z., Bian X., Liang Y., Influence of Different Vinyl Acetate Contents on the Properties of the Copolymer of Ethylene and Vinyl Acetate/Modified Nano-SiO₂ Composite Pour-Point Depressant, Energy & Fuels 31(6) (2017) 5854-5859. doi: 10.1021/acs.energyfuels.7b00189.
[22] Sun Z., Jing G., Tu Z., Effect of modified nano-silica/EVA on flow behavior and wax crystallization of model oils with different wax contents, Journal of Dispersion Science and Technology 39(1) (2017) 71-76. doi: 10.1080/01932691.2017.1295869.
[23] Al-Sabagh A.M., Betiha M.A., Osman D.I., Hashim A.I., El-Sukkary M.M., Mahmoud T., A new covalent strategy for functionalized montmorillonite–poly(methyl methacrylate) for improving the flowability of crude oil, RSC Advances 6(111) (2016) 109460-109472. doi: 10.1039/c6ra21319g.
[24] Yao B., Li C., Yang F., Sjöblom J., Zhang Y., Norrman J., Paso K., Xiao Z., Organically modified nano-clay facilitates pour point depressing activity of polyoctadecylacrylate, Fuel 166 (2016) 96-105. doi: 10.1016/j.fuel.2015.10.114.
[25] Arrighi V., McEwen I.J., Qian H., Serrano Prieto M.B., The glass transition and interfacial layer in styrene-butadiene rubber containing silica nanofiller, Polymer 44(20) (2003) 6259-6266. doi: 10.1016/s0032-3861(03)00667-0.
[26] Landry C.J.T., Coltrain B.K., Landry M.R., Fitzgerald J.J., Long V.K., Poly(vinyl acetate)/silica-filled materials: material properties of in situ vs fumed silica particles, Macromolecules 26(14) (1993) 3702-3712. doi: 10.1021/ma00066a032.
[27] Ahmed H.A., Mubarak M.F., Adsorption of Cationic Dye Using A newly Synthesized CaNiFe2O4/Chitosan Magnetic Nanocomposite: Kinetic and Isotherm Studies, J. Polym. Environ. 29(6) (2021) 1835-1851. doi: 10.1007/s10924-020-01989-0.
[28] Yui-U S., Skorokhodov S.S., Vansheidt A.A., Copolymerization of N-vinylaacetanilide with vinylacetate and styrene, Polymer Science U.S.S.R. 6(7) (1964) 1426-1429. doi: 10.1016/0032-3950(64)90149-2.
[29] Diaz-Calleja R., Riande E., Roman J.S., Compan V., Relaxation Processes in Poly(2-chlorocyclohexyl acrylate) As Studied by Dielectric Relaxation and Mechanical Relaxation Spectroscopy, Macromolecules 28(2) (1995) 614-621. doi: 10.1021/ma00106a029.
[30] Hernández M., Carretero-González J., Verdejo R., Ezquerra T.A., López-Manchado M.A., Molecular Dynamics of Natural Rubber/Layered Silicate Nanocomposites As Studied by Dielectric Relaxation Spectroscopy, Macromolecules 43(2) (2009) 643-651. doi: 10.1021/ma902379t.
[31] Qu M., Deng F., Kalkhoran S.M., Gouldstone A., Robisson A., Van Vliet K.J., Nanoscale visualization and multiscale mechanical implications of bound rubber interphases in rubber–carbon black nanocomposites, Soft Matter 7(3) (2011) 1066-1077. doi: 10.1039/c0sm00645a.
[32] Roy M., Nelson J.K., MacCrone R.K., Schadler L.S., Reed C.W., Keefe R., Zenger W., Polymer nanocomposite dielectrics - the role of the interface, IEEE Transactions on Dielectrics and Electrical Insulation 12(4) (2005) 629-643. doi: 10.1109/tdei.2005.1511089.
[33] Utracki L., Clay-containing polymeric nanocomposites and their properties, IEEE Electrical Insulation Magazine 26(4) (2010) 8-15. doi: 10.1109/mei.2010.5511184.
[34] Vo L.T., Anastasiadis S.H., Giannelis E.P., Dielectric study of Poly(styrene-co-butadiene) Composites with Carbon Black, Silica, and Nanoclay, Macromolecules 44(15) (2011) 6162-6171. doi: 10.1021/ma200044c.
[35] Chen H., Hassan M.K., Peddini S.K., Mauritz K.A., Macromolecular dynamics of sulfonated poly(styrene-b-ethylene-ran-butylene-b-styrene) block copolymers by broadband dielectric spectroscopy, European Polymer Journal 47(10) (2011) 1936-1948. doi: 10.1016/j.eurpolymj.2011.07.005.
[36] Huimin W., Minghua M., Yongcai J., Qingshan L., Xiaohong Z., Shikang W., A study on the preparation of polymer/montmorillonite nano-composite materials by photo-polymerization,

Polymer International 51(1) (2001) 7-11. doi: 10.1002/pi.757.
[37] Elbanna S.A., Abd El Rhman A.M.M., Al-Hussaini A.S., Khalil S.A., Synthesis and characterization of polymeric additives based on α-Olefin as pour point depressant for Egyptian waxy crude oil, Petroleum Science and Technology 35(10) (2017) 1047-1054. doi: 10.1080/10916466.2017.1307852.
[38] Elbanna S.A., Abd El Rhman A.M.M., Al-Hussaini A.S., Khalil S.A., Synthesis, characterization, and performance evaluation of novel terpolymers as pour point depressors and paraffin inhibitors for Egyptian waxy crude oil, Petroleum Science and Technology 40(18) (2022) 2263-2283. doi: 10.1080/10916466.2022.2041660.
[39] Elbanna S.A., Abd El Rhman A.M.M., Al-Hussaini A.S., Khalil S.A., Paraffin inhibition and pour point depression of waxy crude oil using newly synthesized terpolymeric additives, Egyptian Journal of Chemistry (2022) -. doi: 10.21608/ejchem.2022.132291.5838.
[40] Elbanna S.A., Abd El Rhman A.M.M., Al-Hussaini A.S., Khalil S.A., Development of Novel Terpolymes and Evaluating Their Performance as Pour Point Depressants and Paraffin Inhibitors for Waxy Crude Oil, Egyptian Journal of Chemistry (2022) -. doi: 10.21608/ejchem.2022.120528.5414.
[41] A. A R., A. Sayed M., Elbanna S.A., Hafez E., Roushdi M., abdelrahaman a., Effect of solid contents and the ratio of EVA/ Octadecylacrylate blends on Paraffin Inhibition and pour point temperature of waxy crude oil, Egyptian Journal of Chemistry 0(0) (2021) 0-0. doi: 10.21608/ejchem.2021.70234.3547.
[42] Lei Q., Zhang F., Guan B., Liu G., Li X., Zhu Z., Influence of shear on rheology of the crude oil treated by flow improver, Energy Reports 5 (2019) 1156-1162. doi: 10.1016/j.egyr.2019.08.009.
[43] Osmani R., Tahiri A., Fiscal Decentralization and Local Employment Growth: Empirical evidence from Kosovo's municipalities, SERIES V - ECONOMIC SCIENCES (2022) 63-74. doi: 10.31926/but.es.2022.15.64.1.7.
[44] Ren Y., Chen Z., Du H., Fang L., Zhang X., Preparation and Evaluation of Modified Ethylene–Vinyl Acetate Copolymer as Pour Point Depressant and Flow Improver for Jianghan Crude Oil, Industrial & Engineering Chemistry Research 56(39) (2017) 11161-11166. doi: 10.1021/acs.iecr.7b02929.
[45] Tinsley J.F., Jahnke J.P., Adamson D.H., Guo X., Amin D., Kriegel R., Saini R., Dettman H.D., Prud'home R.K., Waxy Gels with Asphaltenes 2: Use of Wax Control Polymers, Energy & Fuels 23(4) (2009) 2065-2074. doi: 10.1021/ef800651d.
[46] Yao B., Li C., Mu Z., Zhang X., Yang F., Sun G., Zhao Y., Ethylene-Vinyl Acetate Copolymer (EVA) and Resin-Stabilized Asphaltenes Synergistically Improve the Flow Behavior of Model Waxy Oils. 3. Effect of Vinyl Acetate Content, Energy & Fuels 32(8) (2018) 8374-8382. doi: 10.1021/acs.energyfuels.8b01937.
[47] Yao B., Li C., Yang F., Zhang X., Mu Z., Sun G., Zhao Y., Ethylene–Vinyl Acetate Copolymer and Resin-Stabilized Asphaltenes Synergistically Improve the Flow Behavior of Model Waxy Oils. 1. Effect of Wax Content and the Synergistic Mechanism, Energy & Fuels 32(2) (2018) 1567-1578. doi: 10.1021/acs.energyfuels.7b03657.
[48] Bestmann H.J., Book Review: Elementary Practical Organic Chemistry. Part 2. Qualitative Organic Analysis. By A. I. Vogel, Angewandte Chemie International Edition in English 6(12) (1967) 1091-1092. doi: 10.1002/anie.196710913.
[49] Sharma S., Srivastava A.K., Synthesis and characterization of copolymers of limonene with styrene initiated by azobisisobutyronitrile, European Polymer Journal 40(9) (2004) 2235-2240. doi: 10.1016/j.eurpolymj.2004.02.028.
[50] Yang F., Paso K., Norrman J., Li C., Oschmann H., Sjöblom J., Hydrophilic Nanoparticles Facilitate Wax Inhibition, Energy & Fuels 29(3) (2015) 1368-1374. doi: 10.1021/ef502392g.
[51] Ahmed H.A., Elbanna S.A., Khalil R., Tayel A., El Basaty A.B., Ultrasonic-assisted Hydrothermal Synthesis of Zeolite Y Adsorbent from Natural Kaolin for the Recycling of Waste Engine Oil, Egyptian Journal of Chemistry 65(13) (2022) -. doi: 10.21608/ejchem.2022.106134.4879.
[52] Ahmed H.A., Altalhi A.A., Elbanna S.A., El-Saied H.A., Farag A.A., Negm N.A., Mohamed E.A., Effect of Reaction Parameters on Catalytic Pyrolysis of Waste Cooking Oil for Production of Sustainable Biodiesel and Biojet by Functionalized Montmorillonite/Chitosan Nanocomposites, ACS Omega 7(5) (2022) 4585-4594. doi: 10.1021/acsomega.1c06518.
[53] Ahmed H.A., Soliman M.S.S., Othman S.A., Synthesis and Characterization of Magnetic Nickel Ferrite-Modified Montmorillonite Nanocomposite For Cu (II) and Zn (II) Ions Removal From Wastewater, Egyptian Journal of Chemistry 0(0) (2021) 0-0. doi: 10.21608/ejchem.2021.69597.3527.
[54] Hanafi S.A., Elmelawy M.S., Ahmed H.A., Solvent-free deoxygenation of low-cost fat to produce diesel-like hydrocarbons over Ni–MoS2/Al2O3–TiO2 heterogenized catalyst, International Journal of Energy and Water Resources 6(1) (2021) 1-13. doi: 10.1007/s42108-021-00156-y.
[55] Ahmed H.A., Elbanna S.A., Khalil R., Tayel A., El Basaty A.B., Ultrasonic-assisted Hydrothermal Synthesis of Zeolite Y Adsorbent from Natural Kaolin for the Recycling of Waste Engine Oil, Egyptian Journal of Chemistry 0(0) (2022) 0-0. doi: 10.21608/ejchem.2022.106134.4879.
[56] Elarbe B., Elganidi I., Ridzuan N., Yusoh K., Abdullah N., Vijayakumar S., Synthesis, characterization and evaluation of stearyl acrylate-co-behenyl acrylate copolymer as a pour point depressant of waxy crude oil, Journal of Petroleum Exploration and Production Technology 12(7) (2021) 1811-1828. doi: 10.1007/s13202-021-01408-7.

[57] Solyman S.M., Aboul-Gheit N.A.K., Sadek M., Tawfik F.M., Ahmed H.A., The effect of physical and chemical treatment on nano-zeolite characterization and their performance in dimethyl ether preparation, Egyptian Journal of Petroleum 24(3) (2015) 289-297. doi: 10.1016/j.ejpe.2015.07.007.
[58] Solyman S.M., Aboul-Gheit N.A.K., Tawfik F.M., Sadek M., Ahmed H.A., Performance of ultrasonic – Treated nano-zeolites employed in the preparation of dimethyl ether, Egyptian Journal of Petroleum 22(1) (2013) 91-99. doi: 10.1016/j.ejpe.2012.09.003.
[59] Garg U., Kaur M.P., Jawa G.K., Sud D., Garg V.K., Removal of cadmium (II) from aqueous solutions by adsorption on agricultural waste biomass, Journal of Hazardous Materials 154(1-3) (2008) 1149-1157. doi: 10.1016/j.jhazmat.2007.11.040.
[60] Chindaprasirt P., Rattanasak U., Eco-production of silica from sugarcane bagasse ash for use as a photochromic pigment filler, Sci. Rep. 10(1) (2020) 9890-9890. doi: 10.1038/s41598-020-66885-y.
[61] Ercegkuzmic A., Radosevic M., Bogdanic G., Srica V., Vukovic R., Studies on the influence of long chain acrylic esters polymers with polar monomers as crude oil flow improver additives, Fuel 87(13-14) (2008) 2943-2950. doi: 10.1016/j.fuel.2008.04.006.
[62] Gou S., Luo S., Liu T., Xia H., Jing D., Zhang Q., Li S., Li Z., Guo Q., Thermally stable imidazoline-based sulfonate copolymers for enhanced oil recovery, RSC Advances 5(104) (2015) 85165-85173. doi: 10.1039/c5ra15434k.
[63] Lai N., Dong W., Ye Z., Dong J., Qin X., Chen W., Chen K., A water-soluble acrylamide hydrophobically associating polymer: Synthesis, characterization, and properties as EOR chemical, Journal of Applied Polymer Science 129(4) (2012) 1888-1896. doi: 10.1002/app.38893.
[64] Wu Y., Ni G., Yang F., Li C., Dong G., Modified Maleic Anhydride Co-polymers as Pour-Point Depressants and Their Effects on Waxy Crude Oil Rheology, Energy & Fuels 26(2) (2012) 995-1001. doi: 10.1021/ef201444b.
[65] Yao B., Mu Z., Li C., Yang F., Zhang X., Effective flow improving agents for waxy crude oil, Petroleum Science and Technology 35(17) (2017) 1775-1783. doi: 10.1080/10916466.2017.1375947.
[66] Ren H., Sun J., Wu B., Zhou Q., Synthesis and characterization of a novel epoxy resin containing naphthyl/dicyclopentadiene moieties and its cured polymer, Polymer 47(25) (2006) 8309-8316. doi: 10.1016/j.polymer.2006.09.070.
[67] Sharma R., Mahto V., Vuthaluru H., Synthesis of PMMA/modified graphene oxide nanocomposite pour point depressant and its effect on the flow properties of Indian waxy crude oil, Fuel 235 (2019) 1245-1259. doi: 10.1016/j.fuel.2018.08.125.
[68] Elbanna S.A., Abd El Rhman A.M.M., Al-Hussaini A.S., Khalil S.A., Development of Novel Terpolymes and Evaluating Their Performance as Pour Point Depressants and Paraffin Inhibitors for Waxy Crude Oil, Egyptian Journal of Chemistry 66(1) (2023) 63-72. doi: 10.21608/ejchem.2022.120528.5414.
[69] Huang H., Wang W., Peng Z., Ding Y., Li K., Li Q., Gong J., The influence of nanocomposite pour point depressant on the crystallization of waxy oil, Fuel 221 (2018) 257-268. doi: 10.1016/j.fuel.2018.01.040.
[70] Li N., Mao G., Wu W., Liu Y., Effect evaluation of ethylene vinyl acetate/nano-montmorillonite pour-point depressant on improving the flow properties of model oil, Colloids and Surfaces A: Physicochemical and Engineering Aspects 555 (2018) 296-303. doi: 10.1016/j.colsurfa.2018.06.065.